DOI: https://doi.org/10.26896/1028-6861-2023-89-3-70-79

PROBABILITY OF FAILURE OF A PIPE EXPOSED TO SEISMIC DISPLACEMENT AND INTERNAL PRESSURE

© Jean-Pierre Ahonsu Komla, Guy Pluvinage*, Julien Capelle

LEM3 — ENIM — University of Lorraine, 57070, Metz, France; *e-mail; pluvinage.guy@orange.fr

Received August 29, 2022. Revised August 29, 2022. Accepted October 2, 2022.

The failure probability and the reliability index have been determined for a pipe submitted to internal pressure, exhibiting a corrosion defect, embedded in a soil with a ground reaction, and underwent the displacement due to seismic activity. Results are obtained by computing the condition of failure: strain demand higher than strain resistance which is typically the Strain Based Design (SBD) basis. From the probabilistic point of view, this condition results in the overlay of the two probability distributions, namely, demand and resistance. An analytical method is proposed to compute the common area between the strain demand and resistance distribution and then to get the probability of failure. The strain demand is assumed to follow a power-law distribution and the strain resistance is a Normal one. The strain demand is computed assuming that the probability density of seismic waves follows a Gutenberg – Richter distribution law. This simple method is also used to predict the failure probability of different reference periods or seismic zone. It is also used to examine the influence of the coefficient of variation of the strain resistance distribution when using vintage pipe steels.

Keywords: pipe; defects; seismic displacement; internal pressure; probability of failure; strain based design; safety factor.

Introduction

The failure risk assessment can be done in two ways, one determinist and the second probabilistic. In a deterministic approach, one compares the safety factor to a prescribed value. For a probabilistic one, the failure probability is compared to a conventional value. The safety factor is defined as the ratio of the resistance and the demand.

A more precise definition depends based on the stress-based design (SyBD) or strain-based design (SBD) [1, 2].

For a stress-based design, the safety factor is defined as the ratio of the yield stress σ_y and the stress demand σ_d . For SBD, the safety factor is the

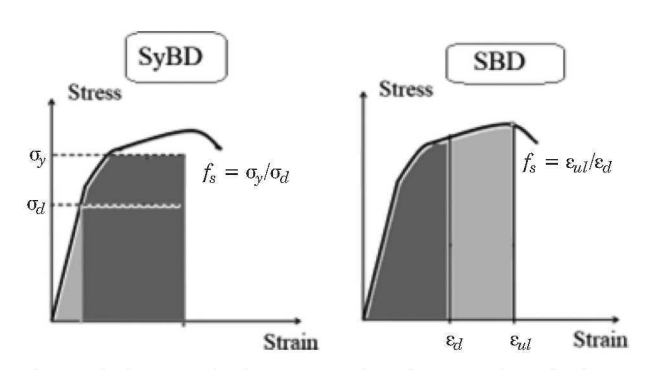


Fig. 1. Schema of the principle of stress-based design (SyBD) and strain-based design (SDB): yield stress σ_y , stress demand σ_d , strain demand ε_d , and ultimate strength ε_{ul}

ratio of the ultimate strain and the strain demand as illustrated in Fig. 1.

For a probabilistic approach, either SyBD or SBD, the safety factor is defined from the statistical distribution of the resistance and the demand more precisely as the ratio of the mean value of the resistance μ_R and the mean value of the demand μ_d :

$$f_s = \mu_R/\mu_d. \tag{1}$$

The prescribed value of the safety factor is generally $f_s = 2$ for SyBD. The earliest information about the use of this value is given in the code of Hammurabi (Codex Hammurabi). The best preserved ancient law code was created in 1760 bc in ancient Babylon. It was enacted by the sixth Babylonian king, Hammurabi. The text covers the bottom portion of a basalt stele with the laws written in cuneiform script. It contains a list of crimes and their various punishments, as well as settlements for common disputes and guidelines for citizen conduct. It is mentioned that an architect, who built a house that collapsed on its occupants and caused their deaths, is condemned to capital punishment. In addition, it is noted that "when a stone is necessary to build a palace, the architect has to plan to use two stones." This was the first information about the value of 2 for the safety factor.

Density probability functions

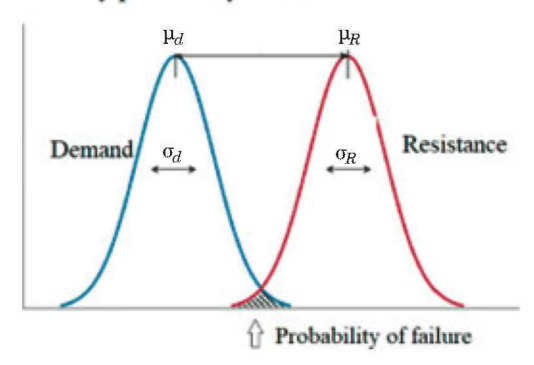


Fig. 2. Definition of the probability of failure

In codes that specifically allow strain-based design (DNV 2000, DNV-OS-F101 [3] ASME B31 [4], CSA Z662 [5] AND API 1104 [6]), the safety factor is a deterministic one $f_{s,det}$ and generally established by expert judgments. Table 1 gives the deterministic safety factors according to the safety classes for tension.

For failure risk, the admissible probability $P_{f,ad}$ has to be less than a conventional value which depends on the types of risk and equipment. If there is no human risk $P_{f,ad}=10^{-4}$, with human risk $P_{f,ad}=10^{-5}$ and for nuclear components $P_{f,ad}=10^{-6}$. This conventional value is a compromise between the cost and the risk [7]. For pipes, the traditional value is $P_{f,ad}=10^{-5}$.

The resistance (R) and the demand (d) functions involve random variable (s) with different density probability distribution functions (PDF). One assumes that the resistance (R) and the demand (d) are independent variables with respective PDF p_d and p_R . The failure probability is represented by the overlay of these PDFs as indicated in Fig. 2 [8].

A reliability index is an attempt to quantitatively assess the reliability of a system using a single numerical value. The set of reliability indices varies depending on the field of engineering, and multiple different indices may be used to characterize a single system. The loss of load probability (LOLP) reflects the probability of the demand exceeding the capacity in a given interval of time (for example, a year) before any emergency measures are taken. It is defined as a percentage of time during which the load on the system exceeds its capacity.

If X is the performance of interest and if X is a Normal random variable, the failure probability is computed by $P_f = \Phi(-\gamma)$, γ is the reliability index. When X is a nonlinear function of n normal random variables $(X_1, ..., X_n)$, then the preceding formula can be generalized, with some approximation. One uses a nice property of the reliability index,



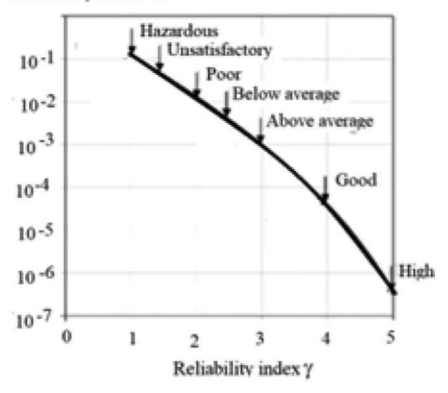


Fig. 3. USACE (1997) guidelines for reliability index and the corresponding probability of failure [10]

to be the shortest distance of the origin to the failure region. This value is computed in FORM and SORM methods [9].

USACE [10] made specific recommendations on target reliability indices in geotechnical and infrastructure projects, Fig. 3.

When additional and accidental loading generated by either permanent or transient ground deformation are superimposed on the internal pressure of a gas or oil pipe, large stresses and strains are produced in the pipe wall. Seismic activity, soil subsidence, slope instability, frost heave, thermal expansion and contraction, landslides, pipe reeling, pipe laying, and other types of environmental loading can be caused by these additional loadings. In these cases, the stresses and strains exceed the proportional limit. For such loading cases, the Strain Based Design (SBD) is the most appropriate one [1].

Displacements due to seism are obtained from Eurocode 8 [11] which gives these displacements as a function of the criticality of the seismic zone on the Richter scale. The distribution of the seism amplitude is given by a distribution of Gutenberg – Richter [12]. The Gutenberg – Richter law (GR law) expresses the relationship between the magnitude and total number of earthquakes in any given region and period.

In this paper, the probability of failure of a pipe submitted to stochastic displacements due to a seism is calculated according to the method of overlapping the demand and the resistance distribution. This pipe exhibits a corrosion defect which is for a conservative reason, considers a semi-ellipti-

Table 1. Safety factors according to the safety classes

Strain safety		Class	
factor	Low	Normal	High
Safety class	1.5	2	3

Table 2. Chemical composition of API 5L X60 steel

Additives	C	Si	Mn	P	S	V	Nb	Ti
%	0.16	0.45	1.65	0.020	0.010	0.07	0.05	0.04

cal defect. This defect is considered a stress concentrator. Therefore a local approach is necessary and the strain resistance is considered as the local effective critical strain $\varepsilon_{ef,c}$. The effective critical strain takes into account the sensitivity of the critical strain to stress triaxiality β and Lode angle θ_l according to the Wierzbicki and Xue [13] model. The distribution of this local critical strain is assumed to follow a Normal distribution. The demand distribution is assumed to follow the French "low" GR distribution.

The two distributions (the local strain demand and the local strain resistance) allow computing the probability of failure and reliability index according to the seismic zone. The influence of the coefficient of variation of the resistance distribution particularly for vintage pipe steels and the expected life duration of the pipeline is also studied.

Effective critical strain according to Wierzbicki and Xue model [10]

It has been seen that failure resistance is sensitive to stress triaxiality β [14 – 19] and Lode angle θ_l [20 – 22]. The influence of stress triaxiality and Lode angle is taken into account in the Mohr – Coulomb (MMC) fracture criterion [23]

$$\begin{split} \varepsilon_{ef,c}(\beta,\theta_{l}) &= \frac{C_{0}}{C_{2}} \left[C_{3} + \frac{\sqrt{3}}{2 - \sqrt{3}} (1 - C_{3}) \sin \frac{\pi \theta_{l}}{6} \right] \times \\ &\times \left[\sqrt{\frac{1 + C_{1}^{2}}{3}} \cos \frac{\pi \theta_{l}}{6} + C_{1} \left(\beta + \frac{1}{3} \right) \sin \frac{\pi \theta_{l}}{6} \right], \end{split} \tag{2}$$

where C_0 , C_1 , C_2 , and C_3 are material constants. Here, the influence of β and θ_l on effective failure

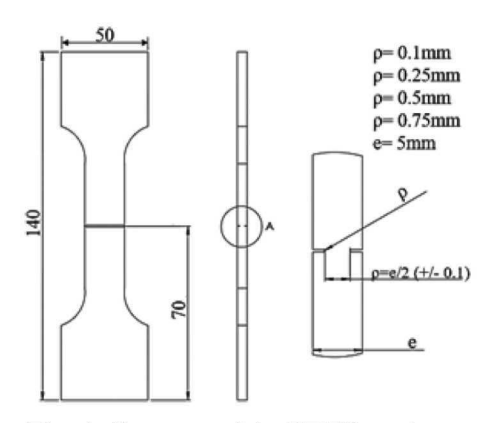


Fig. 4. Geometry of the DENT specimens

strain ε_{efc} is more simply described according to the Wierzbicki and Xue model [13]:

$$\varepsilon_{ef,c}(\beta, \theta_l) = \varepsilon_R^0 \mu_B(\beta) \mu_{\theta_l}(\theta_l),$$
(3)

 ε_R^0 is the reference strain, i.e., the strain resistance for a stress triaxiality and a Lode angle equal to zero ($\beta = 0$; $\theta_l = 0$). The strain dependence to stress triaxiality $\mu_{\beta}(\beta)$ is given by:

$$\mu_{\beta}(\beta) = Be^{-C\beta},$$
(4)

B and *C* are material constants. The strain dependence to Lode angle and is represented by equation [13]:

$$\mu_{\theta_l}(\theta_l) = \delta + (1 - \delta) \left(\frac{6|\theta_l|}{\pi}\right)^k, \tag{5}$$

 δ is a material constant defined by the ratio of the fracture strain between generalized shear $\theta_l = \pi/2$ and generalized tension ($\theta_l = 0$) subjected to the same hydrostatic pressure.

In the following, the API 5L X60 steel pipe is studied. Table 2 shows the chemical composition of this steel. It is composed of 0.16% carbon and several alloying elements, such as titanium and niobium.

The API 5L X60 steel pipe has yield stress $\sigma_y = 510$ MPa, an ultimate strength $\sigma_{ul} = 610$ MPa and a failure elongation A% = 29.1%. The constants B, C, and k of the Wierzbicki and Xue model [13] have been determined from tensile tests on tensile notched specimens and shear tests on smooth specimens (parameter δ).

Four tensile tests have been performed on Double Edge Notch Tensile (DENT) specimens with different notch radius [0.1; 0.25; 0.5; 0.75 mm]. The geometry of specimens is reported in Fig. 4. Elongations at failure of the DENT specimens are reported in Table 3 (mean values of three identical tests).

Table 3. Results of fracture tests on DENT specimens made in API $5L\ X60$ steel pipe

Notch radius, mm	Failure elongation, %	Stress triaxiality
0.75	1.87	0.80
0.5	1.98	0.82
0.25	2.08	0.89
0.1	2.40	0.98

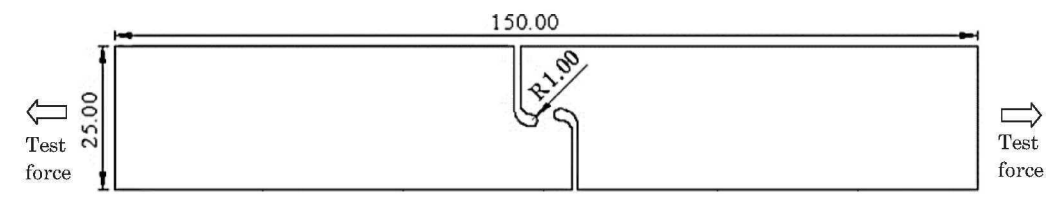


Fig. 5. Geometry of the pure shear specimen

Equation (4) is written with fitted values of parameters C and B:

$$\mu_{\beta}(\beta) = 7.8e^{-1.38\beta}.$$
 (6)

One notes that the value of parameter C = 1.38 is close to the value generally found in literature as C = 1.50 [13, 14].

The material constant δ from equation (5) is obtained from two tests, namely, a shear and a tensile test. The first test gives shear elongation at failure ε_{fs} , and the second one gives tensile elongation at failure ε_f . The δ parameter is given by the ratio of these two failure elongations:

$$\delta = \varepsilon_{f,s}/\varepsilon_f$$
.

The geometry of the pure shear specimen is given in Fig. 5. The values of $\epsilon_{f,s}$, ϵ_f (%), and δ parameter are given in Table 4.

Equation 3 with k=1 (equation (5)) is used to compute the effective strain resistance $\varepsilon_{efc}(\beta, \theta_l)$. The elongation at failure in tension ε_f is a particular case of effective strain resistance

$$\varepsilon_f = \mu_R(\beta = 0.33, \, \theta_l = 0) = 29.1\%.$$
 (7)

This value gives the reference strain resistance $\varepsilon_R^0 = 16.22\%$.

Strain demand distribution of a pipe submitted to internal pressure and seismic loading

A pipe made in steel API 5L X60 with a diameter of 610 mm and a thickness of 11 mm is completely embedded in soil with a ground reaction coefficient of 100 MN/m³ (Fig. 6).

This pipe is submitted to two actions: a 70 bars internal pressure and stochastically local seismic displacement. This displacement is a power function on seism amplitude M (Richter scale) according to [24]:

$$\Delta = 10^{-(4.8 + 0.69M)}. (8)$$

The pipe is clamped at an arbitrary distance of $13 \,\mathrm{m}$ and the local displacement is assumed to be superimposed at an equal distance between two clamped ends. The pipe exhibits a corrosion defect at $3 \,\mathrm{o'clock}$. This defect is considered as a semi-elliptical crack size of depth $d = 0.55 \,\mathrm{mm}$ and

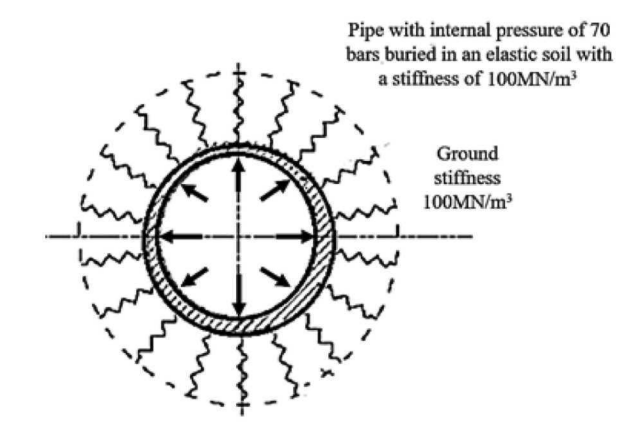


Fig. 6. Embedded pipe in soil with a ground reaction coefficient of 100 MN/m^3

aspect ratio c/e = 18.5/31 = 0.59, where c is the defect semi-axis width and e is the defect semi-axis length.

The local strain resulting from this displacement is computed by the Finite Elements method using Abaqus software. The pipe and the defect are meshing with 3D hexaedric elements Fig. 7.

The stress-strain behavior of the material is assumed to be elastic-plastic. It is obtained from a tensile test and presented as the true stress-strain curve (Fig. 8).

Figure 9 shows an example of the strain distribution ahead of the corrosion defect where the local strain is plotted versus the distance ahead of the defect tip. The effective local strain is obtained from the Volumetric Method (VM) procedure [25] from this strain distribution. Using the VM procedure, the effective distance X_{ef} is determined at the position where the relative stress gradient is minimum. The corresponding value on the strain distribution is the local strain demand according to the concept of the effective strain criterion. This concept assumed that the effective strain is not the maximum strain because the process zone cannot be reduced to one point.

Table 4. Results of shear and tensile test and value of δ

$\epsilon_{f,s}$, %	$arepsilon_f, \%$	δ
6.38	29.1	0.23

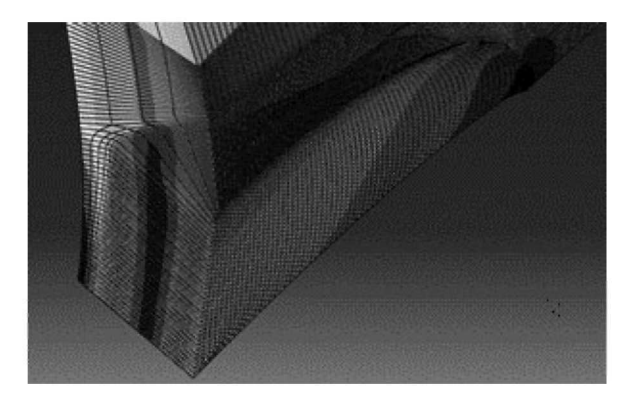


Fig. 7. Meshing in the zone near the crack-like defect

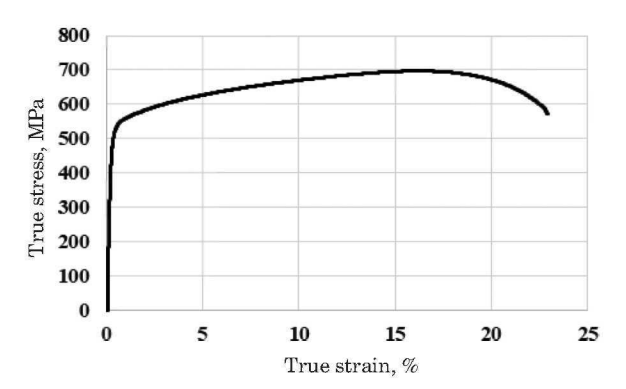


Fig. 8. The true stress-strain curve of API5LX60 pipe steel

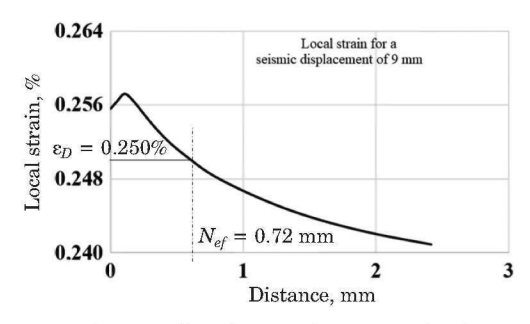


Fig. 9. Local strain distribution for a pipe displacement of 9 mm corresponding to a seismic wave of amplitude M=4

The seismic distribution is described by the Gutenberg – Richter (GR) [12] distribution according to the following equation:

$$N(M) = 10^{a - bM},\tag{9}$$

where N(M) is the number of seismic waves of M amplitude during the observation time (one year).

Table 5. Parameters of the GR seismic distribution in the considered seismic zone [24]

a	b	$M_{ m max}$
0.80	0.60	6.4

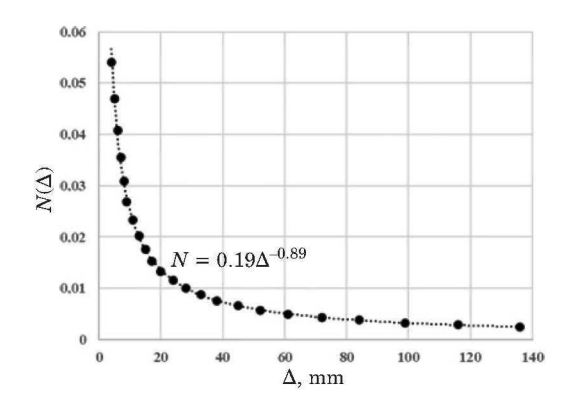


Fig. 10. Displacement distribution due to seismic waves $N = f(\Delta)$

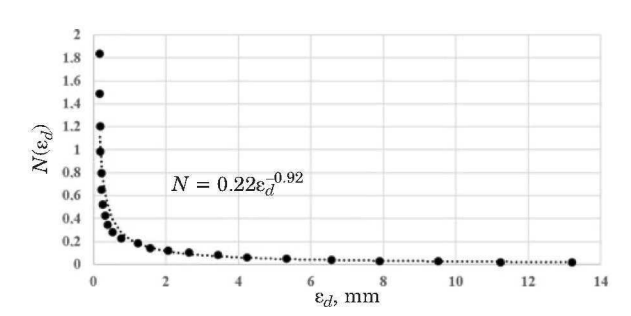


Fig. 11. Strain demand distribution due to seismic waves $N(M) = f(\epsilon_j)$

The GR distribution law is valid for $M < M_{\rm max}$, where $M_{\rm max}$ is the maximum seism amplitude for the considered seismic zone. The parameters of the seismic distribution are given in Table 5.

Figure 10 reports the number of seismic waves of M amplitude versus the corresponding displacement $N(\Delta) = f(\Delta)$ according to the parameters of Table 5 and equation (9):

$$N(M) = f(\Delta) = 0.19\Delta^{-0.89}.$$
 (10)

Figure 11 reports the number of seismic waves of M amplitude versus the local strain demand $N(M) = f(\sigma_d)$:

$$N(M) = 0.22 \varepsilon_J^{-0.92}. \tag{11}$$

The strain demand distribution due to seismic waves $\varepsilon_d = f(M)$ is represented by a power distribution with mean value $\mu_d = 3.16\%$ and standard deviation $\sigma_d = 3.95\%$.

Distribution of the strain resistance

Ten tensile tests have been performed on tensile specimens made with API 5L X60 pipe steel.

Results of failure elongation ε_f are presented in Table 6.

According to the value of kurtosis and skewness, the assumption of a Normal distribution is justified. The coefficient of variation of elongation to failure $COV_{\varepsilon_f} = 0.18$ is higher than those of yield stress $COV_{\sigma_y} = 0.05$.

The strain resistance ε_R is derived from the distribution of failure elongation in tension with a triaxiality $\beta = 0.33$ and a Lode angle $\theta_I = 0$:

$$\varepsilon_f = \varepsilon_R(\beta = 0.33, \, \theta_l = 0). \tag{12}$$

The strain resistance ε_R is computed for a current stress triaxiality β^* which is reported in Fig. 12 versus the displacement Δ . The strain resistance is associated with the studied component and is not a material characteristic. Therefore, it is necessary to compare the strain demand and the strain resistance with the same triaxiality and Lode angle. According to the model of Wierzbicki and Xue [13], the ratio of strain resistance in tension under β^* triaxiality is equal to:

$$\frac{\varepsilon_{R}\left(\beta=0.33\right)}{\varepsilon_{R}\left(\beta=\beta^{*}\right)}=\frac{\mu_{\beta}\left(\beta=0.33\right)\mu_{\theta_{l}}\left(\theta_{l},t\right)}{\mu_{\beta}\left(\beta=\beta^{*}\right)\mu_{\theta_{l}}\left(\theta_{l}^{*}\right)}.\tag{13}$$

The Lode angle in tension is equal to zero and the current Lode angle θ_l^* is close to zero. Therefore, we assume that the Lode angle correction is close to 1.

One notes that in the displacement range [20 – 90 mm] the stress triaxiality is practically constant with an average value $\beta^* = 0.87$. The correction factor is

$$\varepsilon_{R,\beta=\beta^*} = \varepsilon_{R,\beta=0.33} \frac{\exp(-C\beta^*)}{\exp(-0.33C)}$$
 (14)

with C = 1.38. The value of the average correction is 0.47. The statistical parameters of the strain resistance distribution for the studied case are reported in Table 7.

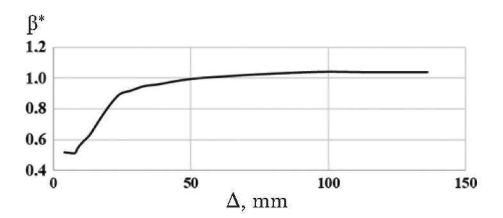


Fig. 12. Evolution of the current stress triaxiality β^* versus displacement Δ

Probability of failure

The difference between the strain demand and the strain resistance represents the failure boundary function (FBF) g(d, R). This FBF is given by

$$g(d, R) = d(\varepsilon_d) - R(\varepsilon_R),$$
 (15)

 $d(\epsilon_d)$ represents the strain demand and $R(\epsilon_R)$ is the strain resistance. The resistance (R) and the demand (d) functions involve random variable(s) with different probability density distribution functions (PDF). One assumes that the resistance (R) and the demand (d) are independent variables with respective PDF p_d and p_R . The failure probability is represented by the overlay of these PDFs as indicated in Fig. 13. The probability of failure is given by:

$$P_{f}[d > R] = \int_{d-R>0}^{R} p_{d,R}(d,R)d(d)dR, \qquad (16)$$

 $p_{d,R}(d,R)$ represents the joint density probability distribution function. In another way the probability of failure P_f is given by the following condition:

$$P_f = P(g < 0). \tag{17}$$

The joint density probability distribution function $p_{d,R}$ has a mean value μ_g and a standard deviation σ_g with:

$$\mu_g = \mu_R - \mu_d,\tag{18}$$

 μ_R , μ_d are the mean values of the resistance and demand distributions, respectively. The standard de-

Table 6. Statistical distribution parameters of elongation to failure of API5L X60

Mean, %	Standard deviation, %	Kurtosis	Skewness	COV	Number of specimens
29.03	5.26	-1.79	0.059	0.18	10

Table 7. Statistical distribution parameters of strain resistance $\varepsilon_{R. \beta = \beta^*}$ of API5L X60

Mean, %	Standard deviation, %	COV	Number of specimens	Kurtosis	Skewness
11.58	4.43	0.396	10	-1.21	$2.75 imes10^{-15}$

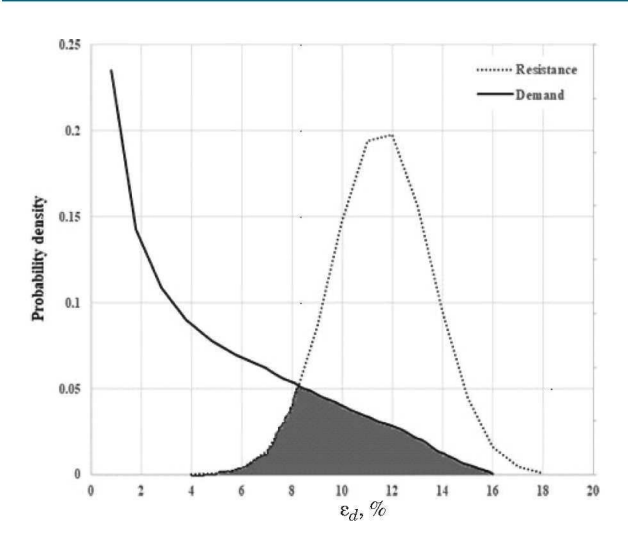


Fig. 13. Failure probability

viation of joint density probability distribution function σ_g is given by:

$$\sigma_g = \sqrt{\sigma_R^2 + \sigma_d^2},\tag{19}$$

 σ_R and σ_d are the standard deviations of the resistance and demand distribution, respectively. The reliability index is defined as the ratio:

$$\gamma = \frac{\mu_g}{\sigma_g} = \frac{\mu_R - \mu_d}{\sqrt{\sigma_R^2 + \sigma_d^2}}.$$
 (20)

Several methods are used for assessing the probability of failure and reliability index. The Monte-Carlo method and the first and second-order reliability methods (FORM and SORM) require derivation of the limit state function. Here, a simple analytical method is proposed assuming that the resistance (R) and the demand (d) density probability functions are represented by simple functions:

$$\begin{split} P_f[g \leq 0] &= P[R-d \leq 0] = \prod_{R < d} P_{d,R}\left(R,d\right) \mathrm{d}R \mathrm{d}(d) = \\ &= \prod_{R < d} P_R\left(R\right) P_d\left(d\right) \mathrm{d}R \mathrm{d}d, \qquad (21) \\ P_f &= \prod_{R < d} P_R\left(R\right) P_d\left(d\right) \mathrm{d}R \mathrm{d}d = \\ &= \prod_{-\infty}^{+\infty} \prod_{-\infty}^{R} P_R\left(R\right) \mathrm{d}R \right] P_d\left(d\right) \mathrm{d}d, \qquad (22) \end{split}$$

$$P_f = \int_{-\infty}^{+\infty} P_R(R) P_d(d) dd. \tag{23}$$

The cumulative probability P_R :

$$P_R(R) = P(R < d). \tag{24}$$

$$P_f = \iint_{R < d} P_R(R) P_d(d) dR dd =$$

$$= \int_{-\infty}^{+\infty} \int_{r}^{+\infty} P_{d}(d) dR P_{R}(dR) dd, \qquad (25)$$

$$P_{f} = \int_{-\infty}^{R} [1 - P_{d}(R)] P_{R}(R) dR.$$
 (26)

The cumulative probability P_d :

$$P_d(R) = P_d(d \le R) = 1 - P_d(d > R),$$
 (27)

$$P_d(\varepsilon_d) = \eta \varepsilon_d^{-\lambda}, \ P_d(R) = 1 - \frac{\eta R^{1-\lambda}}{1-\lambda},$$
 (28)

 η and λ are the parameters of the strain demand distribution. The probability of failure is given by the following equations

$$P_{f} = \int_{0}^{R} \left[1 - \left(1 - \frac{\eta R^{1-\lambda}}{1-\lambda} \right) \right] P_{R}(R) dR, \qquad (29)$$

$$P_{f} = \int_{0}^{+\infty} 1 - \left(1 - \frac{\eta R^{1-\lambda}}{1-\lambda}\right) \frac{1}{\sqrt{2\pi\sigma_{R}}} e^{-\frac{1}{2}\left(\frac{R-\mu_{R}}{\sigma_{R}}\right)^{2}} dR. \quad (30)$$

Equation (30) has been computed using parameters given in Table 7. The GR distribution is limited to M_{max} ($M_{\text{max}} = 6.2$ in our case). The corresponding strain demand is so high that an infinite boundary has been chosen. Values of parameters of equation (30) and the probability of failure are given in Table 8. The failure probability is high when it is compared with recommended values for pipes $P_f < 10^{-5}$. Therefore, a maintenance operation is necessary to repair the corrosion defect. The high values of the failure probability are explained by the intensity of the GR distribution which corresponds to a low seismic zone associated with a severe defect. This defect is considered as not admissible with traditional defect assessment and a deterministic safety factor less than 2.

Table 8. Values of parameters of equation (30) and the probability of failure

μ_R	σ_R	λ	η	P_f
0.115	0.044	0.616	0.0007	1.8×10^{-4}

Table 9. Values of parameters of equations (31) and (32), reliability index and safety factor are given from a new definition

$\mu_R, \%$	$\mu_{d,0.5},\%$	$\sigma_R,\%$	$\sigma_d,\%$	Y*	f_s^*
11.30	3.165	4.47	3.95	1.36	3.57

Table 10. Values of parameters of equations (31) and (32), reliability index and safety factor from clean and vintage steels

Steel	$\mathfrak{p}_R,\%$	$\mu_{d, \ 0.05}, \ \%$	$\sigma_{\!R},\%$	σ_d , %	Υ*	f_s^*
Clean	11.30	3.165	4.47	3.95	1.36	3.57
Vintage	11.30	3.165	5.36	3.95	1.22	3.57

Safety factor

The safety factor f_s [7] is for a stress-based design, generally it is defined by:

$$f_s = \mu_R / \mu_d. \tag{31}$$

The following ratio give the reliability index y:

$$\gamma = \frac{\mu_R - \mu_d}{\sqrt{\sigma_R^2 + \sigma_d^2}}.$$
 (32)

The values of the mean and standard deviation for the demand and the resistance are reported in Table 9.

One notes that the definition of the safety factor (equation (31)) has been established for two Normal distributions and stress-based design. In our case, we compare a Normal distribution with a non-symmetric GR distribution with very high $COV\left(COV_d=1.41\right)$. For this reason, Equation (31) is modified by using the median $\mu_{d,0.5}$ (%). The value of $\mu_{d,0.5}$ is reported also in Table 9

$$f_s = \mu_R / \mu_{d,0.5}. \tag{33}$$

The value of the safety factor is high and associated with a low probability of failure $P_f = 1.8 \times 10^{-4}$. The value of the reliability index γ^* is compared with the value which is given by USACE guidelines for the reliability index [10]. One notes that the situation is between "poor" and "unsatisfactory." This means that the defect must be repaired during a maintenance operation.

Discussion

Influence of the COV of the pipe steel. It is now admitted that the scatter of material properties is also a material property. This scatter is appreciated with the Coefficient of Variation (COV) which is the ratio of the standard deviation and the mean. The COV depends on the studied property of the material. For example, for the pipe steel API5L X60, the COV associated with the elongation of failure is higher than the one associated with yield stress $COV_{\varepsilon_{\tau}} = 18\% > COV_{\sigma_{u}} = 5\%$. The COV

strongly correlates with the microstructure i. e the grain size and the inclusions content. This is the reason that for a vintage pipe steel, the COV_{σ_y} is generally more than two times the value of those of recent and clean pipe steel. The reliability index and the safety factor has been computed using equations (31) and (32) assuming that the standard deviation of a vintage API5L X60 steel is 20% higher than the value of the same clean steel. In this study, the COV of the strain resistance distribution for the vintage pipe steel API5L X60 is $COV_R = 0.39$.

Results are presented in Table 10. One notes a decrease in the reliability index (10%), but the safety factor is unchanged. Therefore, the reliability index associated with the probability of failure is a better representation of the criticality of the situation than the deterministic safety factor.

Influence of the reference period. As indicated in equation (34), the probability distribution of the strain demand follows a power-law:

$$P_d(\varepsilon_d) = \eta \varepsilon_d^{-\lambda},\tag{34}$$

 η and λ the parameters of the strain demand distribution and have been established for a reference period of one year. Assuming that the occurrence of a seismic wave with a magnitude greater than M is proportional to the reference period, the parameter η is proportionally modified for the reference period 10 years and 50 years, and the λ parameter is kept constant, (fifty years is the traditional reference period for a pipe). The probability of failure is computed for the three reference periods (1, 10, and 50 years) and the results are reported in Table 11.

One notes a very strong increase in the failure probability with the increase of the reference period. One concludes the strong necessity of periodic maintenance and repair operations when a pipe is located in a seismic zone.

Influence of seismic zone. France is divided into 4 seismic zones (very low, low, moderate and average) as indicated in Fig. 14. The GR distribution (equation (34)) is different according to the seismic zone. The corresponding GR distribution

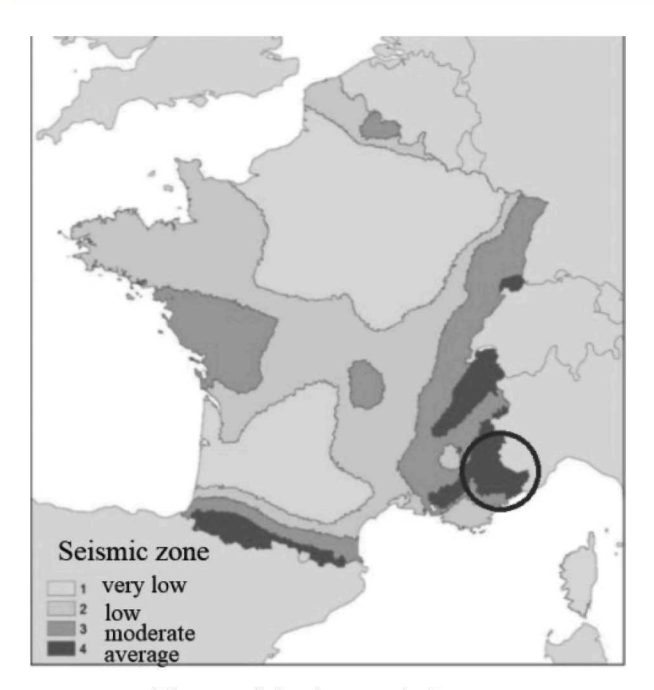


Fig. 14. Seismic zones in France

parameters are reported in Table 12. The studied case corresponds to a "low "seismic zone.

The failure probability for the studied pipe (defect + internal pressure) is sensitive to the seismic zone and only the "very low" seismic zone satisfies the criterion $P_f < 10^{-5}$.

CONCLUSION

Strain Based design is based on a comparison of strain demand and resistance and takes into account material strain hardening. The probability of failure consists to compute the common area of the strain demand and resistance distributions.

A qualitative approach consists also to compute the reliability index (RI) from formulae that incor-

Table 11. Parameters of equation (35) and probability of failure for 3 reference periods

Reference period	λ	ŋ	P_f
1 year	0.62	0.00077	1.8×10^{-4}
10 years	0.62	0.0076	1.7×10^{-3}
50 years	0.62	0.039	10^{-2}

Table 12. Parameters of equation (34) and the probability of failure for 4 seismic zones for the studied pipe

Seismic zone	λ	η	P_f
Very low	0.93	3.87×10^{-5}	9.8×10^{-5}
Low	0.62	0.00077	1.8×10^{-4}
Moderate	0.76	0.0041	2.1×10^{-3}
Average	0.81	0.006	$4.3 imes 10^{-3}$

porate the mean and standard deviation of strain demand and resistance. An acceptable value of RI is given by the probabilistic Model Code (PMC) and is over 3 for a reference period of 50 years. The analytic tool is based on a simple method and the strain demand distribution has been fitted by a simple power function.

In the studied case, the reliability index is between poor and unsatisfactory (1.36), but the loading conditions are severe, however, the seismic distribution is classified as "low," and the corrosion defect is classified as acceptable according to the criterion of fracture mechanics. The proposed tool for probabilistic SBD can be used for the less severe situations.

Improvement of the method can be done using FORM and SORM methods with a loss of simplicity.

REFERENCES

- Pluvinage G. Pipe defect assessment made by strain-based design / Sci. Technol. Oil Oil Prod. Pipeline Transp. 2019. Vol. 9. N 1. P. 67 – 75.
- Kelil Taieb, Amara Mouna, Hadj Meliani Mohammed, Nasser Muthanna Bassam Gamal, Pluvinage G. Assessment of API X65 steel pipe puffiness by a strain-based design (SBD) approach under bi-axial loading / Eng. Failure Anal. 2019. Vol. 104. P. 578 – 588.
- DNV 2000, DNV-OS-F101 Submarine Pipeline Systems, det Norske Veritas, 2000.
- CSA Z662 Oil and Gas Pipeline Systems, Canadian Standards Association 1999.
- ASME B31.8. Gas Transmission, and Distribution Piping Systems. American Society of Mechanical Engineers. — New York, 2012.
- API RP 1111. Design, Construction, Operation and Maintenance of Offshore Hydrocarbon Pipelines (Limit State Design).
 American Petroleum Institute, 1998.
- Pluvinage G. and Sapounov V. Prăvision statistique du comportement des matăriaux / Editor CEPADUES, 2006 [in French].
- Matvienko Yu. G. The simplified approach for estimating probabilistic safety factors in fracture mechanics / Eng. Failure Anal. 2020. Vol. 117. Article 104814.
 DOI: 10.1016/j.engfailanal.2020.104413
- Jallouf Salim. Approache probabiliste du dimensionnement contre le risque de rupture. — Metz: Thesis University of Metz, 2006 [in French].
- USACE 1997. Risk-based analysis in Geotechnical Engineering for Support of Planning Studies, Engineering and Design US Army Corps of Engineers, Department of Army, Washington, DC, 1997. P. 20314-100.
- EN 1998-4. Eurocode 8: design and dimensioning of structures for their resistance to earthquakes. Part 4: silos, tanks, and pipelines (P06-034: 2007-03, NA: 2008-01), 1998.
- Gutenberg B., Richter C. F. Magnitude and Energy of Earthquakes / Ann. Geofis. 1956. N 9. P. 1 – 15.
- Wierzbicki T., Xue L. Ductile fracture initiation and propagation modeling using damage plasticity theory / Eng. Fracture Mech. 2008. P. 3276 – 3293.
- Rice J. R. and Tracey D. M. On the ductile. in triaxial stress fields / J. Mech. Phys. Solids. 1969. Vol. 26. P. 163 – 186.
- 15. Gouair H., Azari Z., Cicliov D et Pluvinage G. Ténacité d'un matériau ductile; un modèle basé sur la distribution locale critique de la deformation / Matér. Techniques. 1995. N 12. P. 7 – 12 [in French].

- Mac Clintock F. A. A Criterion for Ductile Fracture by the Growth of Holes / J. Appl. Mech. 1968. Vol. 35. P. 363.
- Hancock J. W. and Mac Kenzie A. C. On the Mechanisms of Ductile Failure in High-Strength Steels / J. Mech. Phys. Solids. 1976. Vol. 24. P. 47 – 169.
- Dhiab A., Gouair H., Azari Z., Pluvinage G. Dynamic ductile failure of xc18 steel: statistical aspects / Probl. Strength Spec. Publ. 1996. Vol. 96. P. 38 46.
- Griffith. J. R. and Owen. D. R. An elastic plastic stress analysis for a notched bar in plane strain bending / J. Mech. Phys. Solids. 1971. Vol. 19. P. 419 431.
- Barsoum I. and Faleskog J. Rupture mechanisms in combined tension and shear. Experiments / Int. J. Solids Struct. 2007.
 Vol. 44. P. 1768 1786.
- Yingbin Bao, Tomasz Wierzbicki. On fracture locus in the equivalent strain and stress triaxiality space / Int. J. Mech. Sci. 2004. Vol. 46. Issue 1. P. 81 – 98.
- Nahshon K. and Hutchinson J. W. Modification of the Gurson model for shear failure / Eur. J. Mech. A. Solids. 2008.
 Vol. 27. N 1. P. 1 17.
- Paredes M., Wierzbicki T. and Zelenak P. Prediction of crack initiation and propagation in X70 pipeline steel / Eng. Fracture Mech. 2016. Vol. 168. P. 92 – 111.
- BRGM Evaluation probabilistique de l'aléa sismique à l'échelle du territoire national — Etape 3-EPAS3, BRGM/RP-50532-FR. 1997. Novembre [in French].
- 25. Pluvinage G. Fatigue and Fracture emanating from notches. Editor Kluwer, 2003 [in French].